KINETIC STUDY OF PLATELET AGGREGATION

B.-N. MARINCU, MONICA NEAGU, OANA MUNTEANU, A. NEAGU

Department of Biophysics and Medical Informatics, Center for Modeling Biological Systems and Data Analysis, "Victor Babeş" University of Medicine and Pharmaceutics, Timişoara, 2, Piaţa Eftimie Murgu, 300041 Timişoara, Romania; e-mail: neagu@umft.ro

Abstract. Platelet aggregation is important to stop bleeding. In certain pathologies, however, excessive platelet aggregation leads to atherothrombosis and ischemic events. The potentially lethal consequences of impaired platelet aggregation explain the importance of quantitative studies of platelet function. Several techniques have been developed to measure the time course of *in vitro* platelet aggregation induced by agonists such as ADP, epinephrine, collagen, arachidonic acid and ristocetin. Kinetic methods allow for a quantitative analysis of the time-dependence of the aggregation response, and point out the relative importance of the underlying processes. To describe ADP-induced platelet aggregation, we propose a kinetic model that includes three compartments: single platelets, aggregated platelets and deaggregated platelets (i.e. single platelets that have left an aggregate). We assume that deaggregated platelets have different adhesive properties from single platelets that have not been part of an aggregate. Our model is simpler than earlier models, and it is in accord with data obtained by light transmission aggregometry. Applied for healthy subjects and for patients with myeloproliferative disorders (MPD), our kinetic approach suggests that the rate of reaggregation is significantly reduced in MPD.

Key words: light transmission aggregometry, compartmental model, deaggregation, reaggregation, myeloproliferative disorders.

INTRODUCTION

Platelets are anuclear, disk shaped cells that circulate in the blood. Their role is to adhere and aggregate as haemostatic plugs at the site of vascular injury, in order to limit or stop bleeding. Although Bizzozero discovered the role of platelets in intravascular aggregation as early as 1882 [2], it took 80 years until Born developed the method of light transmission aggregometry (LTA), making the first step to uncover their mysteries [3]. LTA has ever since been used in fundamental, clinical and epidemiological investigations.

Received: February 2010;
in final form March 2010.

ROMANIAN J. BIOPHYS., Vol. 20, No. 2, P. 101–114, BUCHAREST, 2010

The right balance of platelet function is vital. On the one hand, if platelets do not adhere properly, surgery is almost impossible; on the other hand, if platelets adhere too much after surgery (e.g. after implantation of artificial heart valves, or after percutaneous coronary interventions), they form potentially lethal blood clots. This is why assessing platelet function is extremely important both for physicians and for pharmaceutical researchers [5].

In order to study platelet function using LTA, blood is drawn by vein puncture and collected with anticoagulants. For calibration of the aggregometer, platelet-poor plasma (PPP) and platelet-rich plasma (PRP) are used. The latter is obtained after centrifugation at 150 g for approximately 15 minutes. The PPP is prepared by centrifuging again at 1200 g for 15 minutes [6]. The kinetics of platelet aggregation is observed using an electric lamp on one side of the PRP-containing cuvette and a photocell on the other: as platelets adhere and bind to one another, the intensity of transmitted light increases.

This method led to the discovery of the first aggregation inhibitors (ATP and adenosine) followed by many others in the years to come. Separated platelets only form aggregates after the addition of agonists that aid the binding of platelets. The most common agonists are adenosine diphosphate (ADP), epinephrine, collagen, ristocetin and the platelet-activating factor (PFA) [5].

Drugs have been discovered in order to prevent platelet aggregation in arterial thrombosis, most prominently in myocardial infarction and stroke, but also after some common surgery. Patients whose thrombotic risk outweighs their risk of bleeding complications are treated with antiplatelet drugs [5]. For example, the dual antiplatelet treatment with aspirin and clopidogrel, which accompanies percutaneous coronary interventions, is under intense investigation because many patients display clopidogrel nonresponsiveness (resistance) [7]. Studies have shown a striking variability in the response to the standard regimen (a 300 mg loading dose followed by a 75 mg daily maintenance dose after stent implantation); about 30% of the patients might not be protected by this regimen and could suffer recurrent ischemic events, including stent thrombosis. Functional and biochemical tests of platelet activity are essential in improving clopidogrel treatment [7, 12].

LTA has been used to evaluate the impact of clopidogrel on platelet function, being considered the gold standard for assessing platelet response to agonists such as adenosine diphosphate (ADP). Nevertheless, LTA is time consuming and requires specially trained technicians, making it difficult to use at the point of care; therefore, several alternative techniques are under investigation [13].

Furthermore, aggregation plays an important part in cell metastasis. Some components of the blood-clotting pathway may facilitate the adhesion of cancerous cells to the endothelium. Thus, an anticoagulant therapy using inhibitors of platelet

aggregation and other substances (such as heparin or the vitamin K inhibitor warfarin) could interfere with this step of the metastatic process [9].

LTA studies have identified specific platelet characteristics, which ease the diagnosis of myeloproliferative diseases. Such characteristics include decreased platelet density, decreased content of serotonin and adenine nucleotides and reduced aggregation response to epinephrine [1, 9].

At low ADP concentrations (below $1\ \mu M$) the aggregation response is transient, whereas at high ADP concentrations (above $10\ \mu M$) aggregation is irreversible at healthy subjects. The maximum aggregation, as well as the steady state value, reached in about 6 minutes (the so-called final aggregation) are ADP concentration dependent; these have been used to characterize platelet function. Maximum aggregation is the most widely reported parameter of platelet function and turned out to be correlated with clinical outcomes [7].

The time course of ADP-induced platelet aggregation can be understood as a result of concurrent aggregation and deaggregation processes. Kinetic studies were used to deconvolute the concurrent processes, i.e. to characterize their contribution to the overall response by the associated rate constants [11]. In these studies, a four-compartment kinetic model has been used [8], in which different compartments are associated to distinct states of the individual platelets.

The present work proposes a three-compartment kinetic model of *in vitro* platelet aggregation induced by ADP and tests it against published experimental data. As a specific example, we use our model to analyze the abnormalities in ADP-induced platelet aggregation observed in chronic myeloproliferative disorders [1].

METHODS

Following the work of Hause *et al*. [8], we describe the aggregation of platelets in PRP on the basis of a compartmental kinetic model.

Here we propose a model with three compartments based on the assumption that, after agonist-induced activation, a platelet may be found in one of the following three states: $S-$ in suspension, not yet aggregated, $A-$ bound in aggregates, $S'-$ in suspension, deaggregated. The latter compartment, S', comprises those platelets that have been part of an aggregate before and have left it, becoming again single platelets in suspension. In what concerns their ability to attach to an aggregate, they differ from activated platelets that have not been part of aggregates [8].

We model transitions between these states using the kinetic scheme

$$S \xrightarrow{k_a} A \underset{k_r}{\overset{k_d}{\rightleftharpoons}} S', \tag{1}$$

where k_a is the rate constant of aggregation, k_d is the rate constant of deaggregation and k_r is the rate constant of reaggregation (i.e. aggregation of individual platelets that have already undergone deaggregation).

The composition of the system will be given by the fractions of cells from each compartment, denoted by x_S, x_A and $x_{S'}$. For example, x_S denotes the number of platelets in compartment S divided by the total number of platelets from the system. According to the kinetic scheme (1), the fractions x_S, x_A and $x_{S'}$ satisfy the system of differential equations

$$\begin{aligned} \frac{\mathrm{d}x_S}{\mathrm{d}t} &= -k_a x_S \\ \frac{\mathrm{d}x_A}{\mathrm{d}t} &= k_a x_S - k_d x_A^{\alpha} + k_r x_{S'}, \\ \frac{\mathrm{d}x_{S'}}{\mathrm{d}t} &= k_d x_A^{\alpha} - k_r x_{S'} \end{aligned} \tag{2}$$

where the exponent α takes into account that deaggregation is an option only for platelets located on the surface of aggregates; platelets deeply buried in aggregates cannot detach from their neighbors.

When the aggregates are small, practically each cell is part of a superficial layer, so $\alpha = 1$ in the differential equations (2), leading to the simple, linear model of platelet aggregation. When the aggregates are large in comparison to the platelet radius, the number of superficial platelets is proportional to the surface area of the aggregate. For spherical aggregates, this is proportional to the square of the aggregate radius; the radius, in turn, is proportional to the power 1/3 of the aggregate volume. Assuming homogeneous packing of platelets within an aggregate, the aggregate volume is proportional to the number of platelets it is composed of. Thus, the number of platelets located on the surfaces of large spherical aggregates is proportional to the power 2/3 of the total number of platelets from those aggregates. Absorbing the proportionality constants in the deaggregation rate constant, k_d, the kinetic equations in this limit will be given by a nonlinear model (2) with $\alpha = 2/3$. Here we will study the solutions of the kinetic equations (2) in these extreme cases, corresponding to aggregate sizes of the order of the platelet diameter ($\alpha = 1$) and much larger than the platelet diameter ($\alpha = 2/3$).

The main contribution to the optical density of the platelet suspension comes from single platelets, i.e. those from compartments S and S' [8, 11]. Thus, the theoretical evolution of the relative optical density (the ratio of the optical density and its initial value) is given by $x_S(t) + x_{S'}(t)$; it is plotted in Fig. 1 for various model parameters. The plots shown in Fig. 1 are in qualitative agreement with aggregation curves obtained by LTA.

Experimental aggregation curves, however, differ in one aspect from the theoretical plots of Fig. 1: they do not start right after the addition of the agonist, since platelet activation also takes time [11]. Therefore, we describe the time course of platelet aggregation by the shifted solution, $OD(t)/OD_0 = x_S(t - t_0) + x_{S'}(t - t_0)$, where $OD(t)$ is the optical density of the suspension at time t and OD_0 is the optical density at the initial moment, t_0. Here t_0 is a model parameter that accounts for the duration of platelet activation. Just as the rate constants, also this parameter is to be obtained by fitting experimental data.

In the case of the linear model ($\alpha = 1$), the theoretical time evolution of the relative optical density, obtained from the analytic solution of Eqs. (2) (see Appendix for details) is given by:

$$\frac{OD(t)}{OD_0} = \frac{k_\mathrm{d}}{k_\mathrm{d} + k_\mathrm{r}} + \left(1 - \frac{k_\mathrm{d}}{k_\mathrm{d} + k_\mathrm{r} - k_\mathrm{a}}\right)\exp\left[-k_\mathrm{a}(t - t_0)\right] + \left(\frac{k_\mathrm{d}}{k_\mathrm{d} + k_\mathrm{r} - k_\mathrm{a}} - \frac{k_\mathrm{d}}{k_\mathrm{d} + k_\mathrm{r}}\right)\exp\left[-(k_\mathrm{d} + k_\mathrm{r})(t - t_0)\right] \tag{3}$$

We tested our kinetic model by fitting published experimental data. Plots of optical density vs. time were digitized using the Matlab function *ginput* (graphical input from mouse). In the case of plots of percent aggregation vs. time [1], we transformed the data into relative optical density by noting that the fraction of aggregated platelets is given by $x_A(t)$; therefore the percent aggregation at time t is $x_A(t) \cdot 100\%$. Since at every instant of time $x_S(t) + x_A(t) + x_{S'}(t) = 1$, the expression of the optical density is $OD(t)/OD_0 = 1 - x_A(t) = 1 - (\text{percent aggregation})/100\%$.

In order to obtain the model parameters (k_a, k_d, k_r, and t_0) we developed a nonlinear least squares program written in Matlab (The MathWorks, Inc., Natick, MA, USA), based on the Nelder-Mead simplex search method, implemented in the *fminsearch* function from Matlab's Optimization Toolbox. Our program is freely available upon e-mail request.

RESULTS

To test the qualitative agreement between experimental data and the theoretical expression obtained by solving Eqs. (2), in Fig. 1 we plotted the theoretical evolution of the platelet suspension's relative optical density for different rate constants. The left panels (A, C, E) depict theoretical aggregation curves that result from the analytic solution of the linear model ($\alpha = 1$), whereas the right panels (B, D, F) result from the numerical solution of the nonlinear model ($\alpha = 2/3$).

Figure 1 shows that both models capture the characteristic features of experimental aggregation curves: they are able to describe reversible aggregation (observed in the case of low agonist concentrations), but also irreversible aggregation (observed in the case of high agonist concentrations) [3, 5, 11].

The rate constants differ in their impacts on two important model-independent parameters that are customarily assessed from experimental aggregation curves: the magnitude of the aggregation response $\Delta OD = OD_0 - OD_{\min}$, and the time to reach maximal aggregation $t_{\text{peak}} = t_1 - t_0$, where t_1 denotes the moment when $OD(t_1) = OD_{\min}$.

The larger the aggregation rate constant k_a, the larger is ΔOD and the smaller is t_{peak} (Figs. 1A and B); as pointed out also in ref. [11], the larger the deaggregation rate constant k_d, the smaller are ΔOD and t_{peak} (Figs. 1 C and D); the larger the reaggregation rate constant k_r, the larger are ΔOD and t_{peak} (Figs. 1, E and F). It is clear from Fig. 1 that each rate constant has a different impact on the curve morphology. Therefore, it is reasonable to expect that the inverse problem, of finding a set of rate constants that optimally describes an aggregation curve, has a unique solution. In the remainder of this paper we will apply a nonlinear least squares procedure to solve the inverse problem in various experimental conditions.

Figure 2 shows fits of LTA data published in the classical paper by Born [3] using the linear model (Fig. 2A) and the nonlinear model (Fig. 2B). Distinct curves correspond to different concentrations of ADP – the agonist used to trigger platelet aggregation. The model parameters that assure the best fit are listed in Table 1. Note that an increase in the ADP concentration increments the rate of reaggregation; the other parameters, however, do not show a monotonous dependence on the ADP concentration.

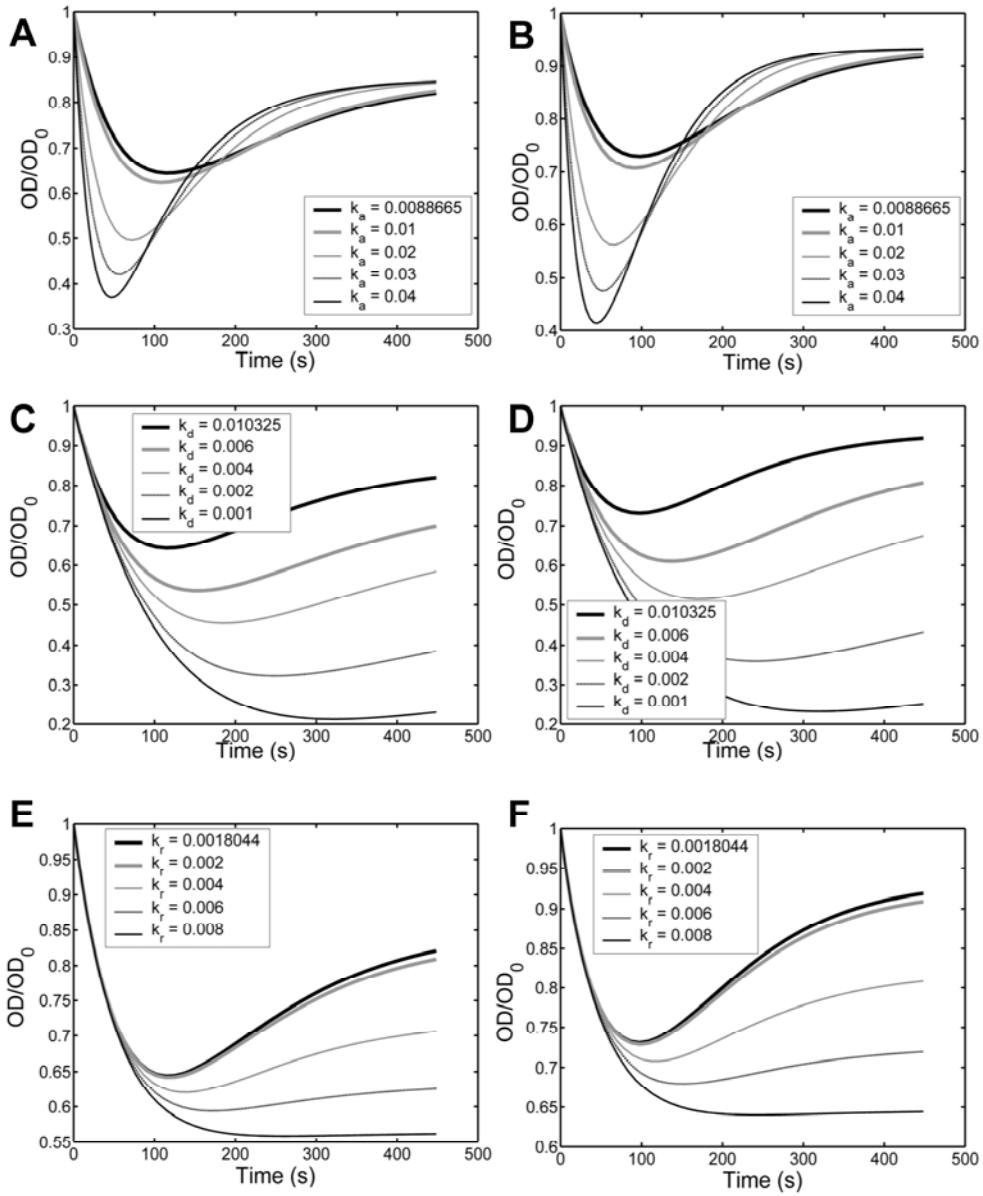

Fig. 1. The time-dependence of the relative optical density obtained from the solution of Eqs. (2) in the linear case, $\alpha = 1$ (A, C, E), and in the nonlinear case, $\alpha = 2/3$ (B, D, F). In all plots, the thick black curves correspond to the set of rate constants $k_a = 8.8665 \times 10^{-3}\,\mathrm{s}^{-1}$, $k_d = 1.0325 \times 10^{-2}\,\mathrm{s}^{-1}$, and $k_r = 1.8044 \times 10^{-3}\,\mathrm{s}^{-1}$; the other curves were obtained by varying just one parameter, as shown in each legend. Aggregation starts at $t_0 = 0$ s.

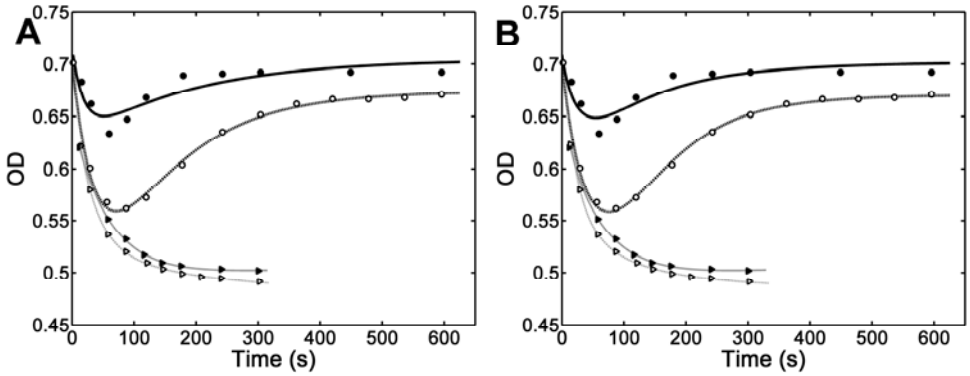

Fig. 2. Markers plot the optical density vs. time during *in vitro* platelet aggregation induced by various concentrations of ADP: 0.25 μM (filled circles), 0.5 μM (open circles), 1 μM (filled triangles), 2.5 μM (open triangles) [3]. Reprinted by permission from [3], Macmillan Publishers Ltd., copyright (1962). The curves result from the least-squares fit of the data using the linear model ($\alpha = 1$ in Eqs. (2)) (A), and the nonlinear model ($\alpha = 2/3$ in Eqs. (2)) (B). See Table 1 for the corresponding parameters.

Table 1

Parameters that resulted from the least squares fit of experimental data obtained by Born [3] using the linear model ($\alpha = 1$ in Eqs. (2)) and the nonlinear model ($\alpha = 2/3$ in Eqs. (2))

Set	t_0 (s)	k_a ($10^{-3}s^{-1}$)	k_d ($10^{-3}s^{-1}$)	k_r ($10^{-3}s^{-1}$)	χ^2	Figure (Plot)
1	0	7.14	47.1	1.92	2.14×10^{-3}	2A (thick solid line)
2	0	10.2	23.4	2.04	2.40×10^{-3}	2A (thick dotted line)
3	11.9	3.50	14.2	3.17	1.31×10^{-5}	2A (thin solid line)
4	13.7	5.80	27.0	7.88	1.36×10^{-5}	2A (thin dotted line)
5	0	8.23	25.6	3.22	1.02×10^{-3}	2B (thick solid line)
6	0	11.0	15.5	3.21	2.46×10^{-3}	2B (thick dotted line)
7	13.7	4.31	9.89	3.85	1.38×10^{-5}	2B (thin solid line)
8	16.6	8.49	23.5	11.0	7.45×10^{-6}	2B (thin dotted line)

Normal platelet aggregation is represented also in Figure 3. Circular markers represent LTA data obtained by Avram *et al*. [1] for healthy subjects. In vitro platelet aggregation is irreversible under these conditions. As shown on Fig. 2 (filled triangles), aggregation is irreversible even for ADP concentrations that are smaller by an order of magnitude than the one corresponding to Fig. 3.

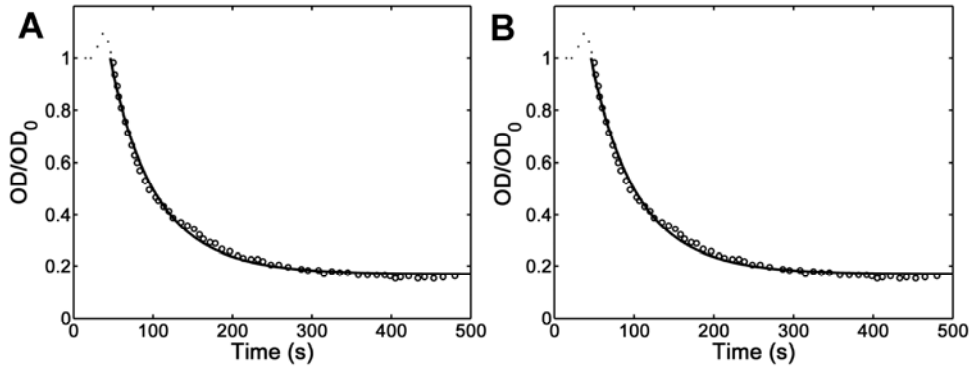

Fig. 3. Markers represent normal platelet aggregation (relative optical density vs. time) in response to the addition of 10 μM ADP (Fig. 1B of ref. [1]), whereas lines represent the best fit of the data by the linear (A) and the nonlinear (B) version of model (1) described by Eqs. (2) with $\alpha = 1$ and $\alpha = 2/3$, respectively. Model parameters are given in Table 2, Sets 1 and 4.

Table 2

Model parameters obtained from the nonlinear least squares fit to experimental data obtained by Avram *et al*. for healthy subjects and for patients with chronic myeloproliferative disorders [1]

Set	t_0 (s)	k_a ($10^{-3}s^{-1}$)	k_d ($10^{-3}s^{-1}$)	k_r ($10^{-3}s^{-1}$)	χ^2	Figure
1	46.1	15.5	7.12	35.3	13.9×10^{-3}	3A
2	55.6	8.67	15.6	1.01	9.36×10^{-4}	4A
3	40.6	10.2	7.06	3.25	5.30×10^{-3}	5A
4	46.0	15.8	5.33	28.0	15.1×10^{-3}	3B
5	55.7	9.52	10.9	2.07	1.38×10^{-3}	4B
6	41.0	11.0	5.81	3.90	4.77×10^{-3}	5B

Certain myeloproliferative disorders, however, lead to impaired platelet function [10], resulting in a smaller magnitude of the aggregation response (ΔOD) and reversible aggregation even in the presence of 10 μM ADP [1]. Figs. 4 and 5 show LTA data obtained by Avram *et al*. [1] for two different patients with chronic myeloproliferative disorders. Although the two curves differ in morphology, our kinetic analysis clearly shows that they have something in common: a reduced rate of reaggregation, smaller by an order of magnitude than in the case of healthy humans (compare Set 1 with Sets 2 and 3 in Table 2).

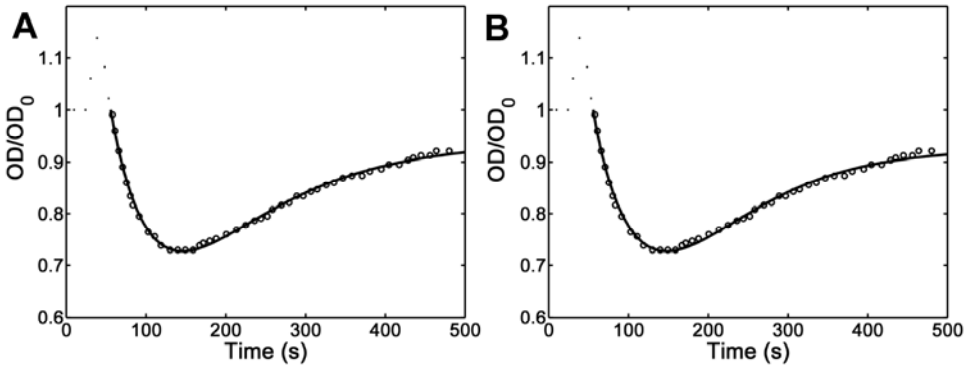

Fig. 4. Markers show the time course of abnormal platelet aggregation observed by Avram *et al*. [1] as a response to 10 μM ADP in certain cases of chronic myeloproliferative disorders (Fig. 4B of ref. [1]). Curves plot the best fit by the linear (A) and the nonlinear (B) version of model (1) described by Eqs. (2) with $\alpha = 1$ and $\alpha = 2/3$, respectively. Parameters are given in Table 2, Sets 2 and 5.

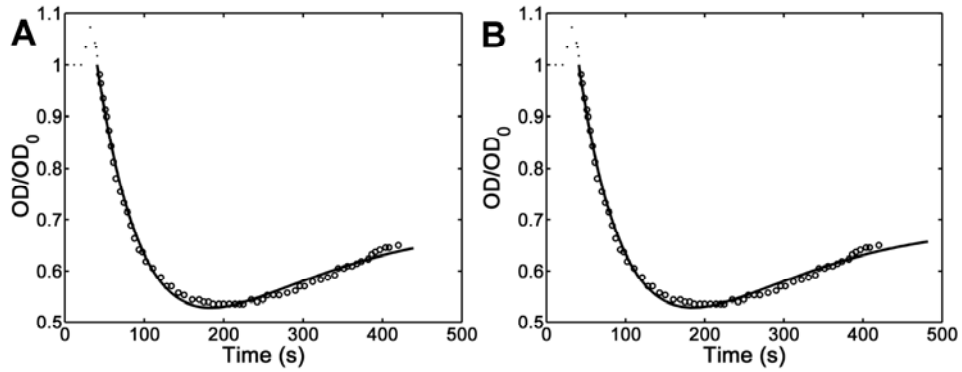

Fig. 5. Markers represent the evolution of the relative optical density of PRP during platelet aggregation induced by 10 μM ADP in the case of a patient that suffers from chronic myeloproliferative disorder (Fig. 5B of ref. [1]). The curves plot the best fit of the data using the linear (A) and the nonlinear (B) version of model (1) (Eqs. (2) with $\alpha = 1$ and $\alpha = 2/3$, respectively). Parameters are given in Table 2, Sets 3 and 6.

DISCUSSION

Throughout this work we used in parallel the solutions of the kinetic equations (2) in the linear case ($\alpha = 1$) and in the nonlinear case ($\alpha = 2/3$). By showing that model (1) fits well the data in both cases, we demonstrated that the kinetics does not change qualitatively because platelets from the bulk cannot leave aggregates.

The expression (3) of the relative optical density obtained from our linear model (Eqs. (2) with $\alpha = 1$) is similar, although not identical, to the analytic formula obtained from a different, four-compartment model [8]. According to the model proposed by Hause *et al*. [8], during the course of aggregation, individual platelets exist in one of four compartments: reactive single platelets that have not yet aggregated (F_0), single platelets that have already dissociated from aggregates (F_1), dissociable aggregates (A_0), and aggregates that cannot dissociate (A_1). Compartments S, A and S'' considered here are precisely compartments, F_0, A_0, and F_1, respectively. The rate constants k_a and k_d are the same as k_1 and k_3 of ref. [8], respectively, whereas k_r plays a similar role to k_2 from the mathematical point of view, but differs from k_2 in interpretation. In our model k_r describes the ability of deaggregated platelets to reattach to aggregates (thereby it is similar to the rate constant k_{-3} neglected in ref. [8]), whereas k_2 describes the transition of aggregated platelets from a dissociable to a non-dissociable state.

The theoretical time-dependence of the relative optical density, that is extensively used to fit and interpret LTA data [11], corresponds to a particular case of the four compartment model of Hause *et al*., in which all reaction steps are irreversible [8].

Our analysis proves that there is no need for compartment A1 in order to describe the experimentally observed kinetics of platelet aggregation.

CONCLUSIONS

We proposed a novel kinetic model of ADP-induced *in vitro* platelet aggregation. Besides the simplest, linear version of the model, we also analyzed a nonlinear version that considers deaggregation only for platelets located on aggregate surfaces. Since the chi-square values are comparable, we conclude that the two models describe experimental data equally well.

The equations of the linear model were solved analytically to obtain the fraction of aggregated platelets at every instant of time; for the nonlinear model a numerical solution was obtained.

Despite the good fit, the value of the deaggregation rate constant is not clearly related to molecular events. In what concerns deaggregation, the linear model (which states that each platelet that is part of an aggregate might deaggregate) is justified when aggregate sizes are of the order of the platelet diameter (at the beginning and, in the case of transient aggregation, also at the end); the nonlinear model is justified when the aggregates are much larger in diameter than a platelet. Nevertheless, kinetic studies based on both models point out the relative importance of the processes involved in the aggregation response.

As a specific application of our kinetic model, we analyzed the abnormalities of ADP-induced platelet aggregation observed in chronic myeloproliferative disorders [1]. While the classical criteria used to analyze curve morphology (maximum aggregation, final aggregation, or the time needed to reach maximum aggregation) did not show a consistent change, the kinetic study clearly indicates that in myeloproliferative disorders the rate of reaggregation is reduced by an order of magnitude. Further kinetic studies of a statistically significant amount of data are needed to firmly prove the impact of myeloproliferative disorders on platelet function.

Although finding the right balance between the benefits and the risks of preventing platelet aggregation is not easy, *in vitro* aggregometry augmented with quantitative data analysis is an important tool in developing new therapies against the main cardiovascular killers.

Acknowledgements. We thank Eugenia Kovács, Viola Popov, Eberhardt Neumann and Tudor Savopol for useful discussions. This paper was supported by the National Agency for Scientific Research under grant CEEX 62/2005.

APPENDIX

Here we briefly derive the analytic solution of the kinetic equations of the linear model (Eq. (2) with $\alpha = 1$). In matrix notations, the equations read:

$$\frac{\mathrm{d}x}{\mathrm{d}t} = \mathbf{K} \times \mathbf{x} \tag{A1}$$

where

$$\mathbf{x}(t) = \begin{bmatrix} x_S(t) \\ x_A(t) \\ x_{S'}(t) \end{bmatrix} \quad \text{and} \quad \mathbf{K} = \begin{bmatrix} -k_\mathrm{a} & 0 & 0 \\ k_\mathrm{a} & -k_\mathrm{d} & k_\mathrm{r} \\ 0 & k_\mathrm{d} & -k_\mathrm{r} \end{bmatrix} \tag{A2}$$

The other symbols are defined in the text related to Eqs. (1) and (2).

Equation (A1) has solutions of the form $\mathbf{x}(t) = v \cdot \exp(\lambda t)$, where λ and the three components of the column matrix v are time-independent real numbers. Substituting this expression into Eq. (A1) we note that it is satisfied only if

$$(\mathbf{K} - \lambda \cdot \mathbf{1}) \cdot v = 0 \tag{A3}$$

in which $\mathbf{1}$ denotes the 3 by 3 unit matrix.

Equation (A3) is known in linear algebra as the eigenvalue problem of matrix $\mathbf{K}$. A system of homogeneous linear equations in the components of v has a solution only if the determinant of the system vanishes:

$$\det(\mathbf{K} - \lambda \cdot \mathbf{1}) = 0\,. \tag{A4}$$

The values of λ obtained by solving Eq. (A4) are the eigenvalues of matrix $\mathbf{K}$; the vector obtained by solving Eq. (A3) for a given eigenvalue λ is the eigenvector of matrix $\mathbf{K}$ that corresponds to the eigenvalue λ.

The third order polynomial equation (A4) has the solutions:

$$\lambda_1 = 0; \qquad \lambda_2 = -k_\mathrm{a}; \qquad \lambda_3 = -(k_\mathrm{d} + k_\mathrm{r}). \tag{A5}$$

By substituting $\lambda = \lambda_1$ into Eq. (A3), and solving this equation for the components of v, we can express each component as a function of one of them. By requiring unit normalization (sum of squares of vector components equal to one), we obtain the normalized eigenvector, v_1, associated to the eigenvalue λ_1. By the same approach applied for each eigenvalue, we obtain the set of three eigenvectors of unit norm:

$$\mathbf{v}_1 = \frac{1}{N_1}\begin{bmatrix} 0 \\ k_\mathrm{r} \\ k_\mathrm{d} \end{bmatrix}; \qquad \mathbf{v}_2 = \frac{1}{N_2}\begin{bmatrix} k_\mathrm{d} + k_\mathrm{r} - k_\mathrm{a} \\ -k_\mathrm{r} + k_\mathrm{a} \\ -k_\mathrm{d} \end{bmatrix}; \qquad \mathbf{v}_3 = \frac{1}{\sqrt{2}}\begin{bmatrix} 0 \\ 1 \\ -1 \end{bmatrix}. \tag{A6}$$

with $N_1 = \sqrt{k_\mathrm{d}^2 + k_\mathrm{r}^2}$ and $N_2 = \sqrt{\left(k_\mathrm{d} + k_\mathrm{r} - k_\mathrm{a}\right)^2 + \left(k_\mathrm{r} - k_\mathrm{a}\right)^2 + k_\mathrm{d}^2}$.

The solution of Eq. (A1) has the general form

$$x(t) = \sum_{i=1}^{3} C_i v_i \exp(-\lambda_i t)\,. \tag{A7}$$

The integration constants C_1, C_2 and C_3 result from the initial condition, $x_S(0) = 1$, $x_A(0) = 0$, and $x_{S'}(0) = 0$; according to Eqs. (A2) and (A7), the initial condition is written as

$$C_1\mathbf{v}_1 + C_2\mathbf{v}_2 + C_3\mathbf{v}_3 = \begin{bmatrix} 1 \\ 0 \\ 0 \end{bmatrix}. \tag{A8}$$

Solving Eq. (A8), we obtain

$$C_1 = \frac{N_1}{k_\mathrm{d} + k_\mathrm{r}}; \quad C_2 = \frac{N_2}{k_\mathrm{d} + k_\mathrm{r} - k_\mathrm{a}}; \quad C_3 = \sqrt{2}\left(\frac{k_\mathrm{d}}{k_\mathrm{d} + k_\mathrm{r}} - \frac{k_\mathrm{d}}{k_\mathrm{d} + k_\mathrm{r} - k_\mathrm{a}}\right). \tag{A9}$$

Combining Eqs. (A5), (A6), (A9) and (A7), we obtain the solution of Eq. (2):

$$x_S(t) = \exp(-k_\mathrm{a} t) \tag{A10a}$$

$$x_A(t) = \frac{k_r}{k_d + k_r} - \frac{k_r - k_a}{k_d + k_r - k_a}\exp(-k_a t) - \left(\frac{k_d}{k_d + k_r - k_a} - \frac{k_d}{k_d + k_r}\right)\exp\left[-(k_d + k_r)t\right] \quad \text{(A10b)}$$

$$x_{S'}(t) = \frac{k_d}{k_d + k_r} - \frac{k_d}{k_d + k_r - k_a}\exp(-k_a t) + \left(\frac{k_d}{k_d + k_r - k_a} - \frac{k_d}{k_d + k_r}\right)\exp\left[-(k_d + k_r)t\right] \quad \text{(A10c)}$$

REFERENCES

1. AVRAM, S., A. LUPU, S. ANGELESCU, N. OLTEANU, D. MUT-POPESCU, Abnormalities of platelet aggregation in chronic myeloproliferative disorders, *J. Cell. Mol. Med.*, 2001, **5**, 79–87.
2. BIZZOZERO, G., Ueber einen neuen Formbestandtheil des Blutes und dessen Rolle bei der Thrombose und der Blutgerinnung, *Arch. Pathol. Anat. Physiol.*, 1882, **90**, 261–332.
3. BORN, G.V.R., Aggregation of blood platelets by adenosine diphosphate and its reversal, *Nature*, 1962, **194**, 927–929.
4. BORN, G.V.R., M.J. Cross, The aggregation of blood platelets, *J. Physiol.*, 1963, **168**, 178–195.
5. BORN, G.V.R., C. PATRONO, Antiplatelet drugs, *Br. J. Pharmacol*, 2006, **147**, 241–251.
6. CATTANEO, M., Platelet aggregation studies: autologous platelet-poor plasma inhibits platelet aggregation when added to platelet-rich plasma to normalize platelet count, *Hematol. J.*, 2007, **92**, 694–697.
7. GURBEL, P.A., U.S. TANTRY, Drug Insight: clopidogrel nonresponsiveness, *Nature Clinical Practice*, 2006, **3**, 387–395.
8. HAUSE, L.L., G.S. RETZINGER, P.A. MEGAN, A compartmental model of platelet aggregation in vitro: the kinetics of single platelets, *Thromb. Res.,* 1989, **56**, 133–146.
9. HEJNA, M., M. RADERER, C.C. ZIELINSKI, Inhibition of metastases by anticoagulants, *J. Natl. Cancer Inst.*, 1999, **91**, 22–36.
10. HOLME, S., S. MURPHY, Platelet abnormalities in myeloproliferative disorders, *Clin. Lab. Med.*, 1990, **10**, 873–888.
11. MAAYANI, S., T.M. TAGLIENTE, T. SCHWARZ, B. CRADDOCK-ROYAL, C. ALCALA, G. MARRERO, R. MARTINEZ, Deaggregation is an integral component of the response of platelets to ADP in vitro: kinetic studies of literature and original data, *Platelets,* 2001, **12**, 279–291.
12. SBRANA, S., F. DELLA PINA, A. RIZZA, M. BUFFA, R. DE FILIPPIS, J. GIANETTI, A. CLERICO, Relationships between optical aggregometry (type Born) and flow cytometry in evaluating ADP-induced platelet activation, *Cytometry Part B (Clinical Cytometry)*, 2008, **74B**, 30–39.
13. WILLIAMS, C.D., G. CHERALA, V. SEREBRUANY, Application of platelet function testing to the bedside, *Thromb. Haemostasis*, 2010, **103**, 29–33.